A COMPARISON OF DIFFERENT TECHNOLOGIES FOR THRUST VECTORING IN A LINEAR AEROSPIKE

MICHELE FERLAUTO[1], ANDREA FERRERO[2], MATTEO MARSICOVETERE[3] AND ROBERTO MARSILIO[4]

[1] Politecnico di Torino
Corso Duca degli Abruzzi 24, 10129 Torino, Italy
michele.ferlauto@polito.it

[2] Politecnico di Torino
Corso Duca degli Abruzzi 24, 10129 Torino, Italy
andrea_ferrero@polito.it

[3] Politecnico di Torino
Corso Duca degli Abruzzi 24, 10129 Torino, Italy
matteo.marsicovetere@studenti.polito.it

[4] Politecnico di Torino
Corso Duca degli Abruzzi 24, 10129 Torino, Italy
roberto.marsilio@polito.it

Key words: Aerospike; Shock Vectoring; Differential Throttling

Abstract. The aerospike nozzle represents an interesting technology for Single-Stage-To-Orbit vehicles because of its self-adapting capability. It is possible to get thrust vectoring capabilities in different ways. A straightforward solution consists in applying differential throttling to multiple combustion chambers which feed the nozzle. An alternative technology, which can be used in the presence of a common combustion chamber, is represented by fluidic thrust vectoring which requires the injection of a secondary flow from a slot on the wall. In this work, the flow field in a linear aerospike nozzle is numerically investigated by means of RANS simulations and both differential throttling and shock vectoring are studied. A parametric study is performed to evaluate the potential of the two technologies.

1 Introduction

Rocket engines used in space launchers are usually equipped with conventional fixed geometry bell shaped nozzle which provide good performances and are quite reliable. However, there are launchers configurations in which there is a core engine which has to work from sea-level to almost vacuum conditions, like the Vulcain 2 engine in the Ariane 5 launcher or the Space Shuttle Main Engines in the Space Shuttle launching system. Furthermore, Single-Stage-to-Orbit (SSTO) configurations have been also proposed. In all these applications a significant performance gain could be obtained by reducing the non-adaptation losses [10].

The aerospike nozzle represents an effective self-adapting nozzle which allows to adapt the nozzle exit pressure according to the environment pressure without the use of any moving component. Several configurations of aerospike engines have been proposed and investigated, with both circular and linear designs [13, 4, 16, 22, 21, 11]. In the 1960s, Rocketdyne developed the J-2T-200K and J-2T-250K annular engines which were based on a toroidal combustion chamber and a truncated plug [19]. These engines, which were derived from the J-2 engine used in the Saturn-family launchers, were evaluated with both cold and hot tests.

The linear aerospike engine XRS-2200 was selected as a candidate propulsion system for the Venture Star/X33 SSTO spaceplane in the 1990s [3].

After these pioneering contributions, the research effort on aerospikes slowed down because of the cancellation of several programs. More recently, the research in field has been lead by universities and private companies [2, 1].

The choice of the aerospike technology requires particular attention when dealing with thrust vectoring. For example, it can be difficult to use a gimballed joint because of the large diameter/extension of aerospike nozzle which prevents the possibility of moving the entire nozzle. However, thrust vectoring is a key requirement for the use of aerospike nozzle in real applications. For these reasons, several alternative thrust vectoring technologies have been investigated [1].

A straightforward control strategy is represented by differential throttling which can be applied in the presence of clustered aerospike engines with multiple independent combustion chamber. Since the mass flow rate and the pressure can be controlled independently in each chamber, it is possible to generate a lateral thrust component which can be used for manoeuvring.

However, there are both annular and linear aerospike configurations in which a common combustion chamber is considered. In this case, differential throttling is no more an option. A possible solution is represented by fluidic thrust vectoring which consists in injecting a secondary flow from the plug wall in order to create an obstacle for the primary flow coming from the throat. This generates a shock followed by a separation downstream to the injection point.

The effectiveness of the fluidic thrust vectoring is influenced by several parameters: injection location, injection mass flow rate, nozzle pressure ratio. These effects have been widely investigated in the literature with both experimental [5, 6, 7] and numerical studies [5, 6, 15, 9, 18, 14].

In the present work, differential throttling and fluidic thrust vectoring are investigated and compared as candidate technologies for thrust control in a linear aerospike. The performances of the control strategies are evaluated in terms of lateral force component magnitude by means of numerical simulations.

2   THRUST IN AN AEROSPIKE NOZZLE

Consider the generic rocket nozzle represented in Figure 1a. The area of the exit section of the nozzle is A_e. The thrust F generated by the rocket can be computed as:

$$F = (F_x, F_y)^T = \int_{A_e} (\rho(u \cdot n)u + (p - p_0)n)dA \tag{1}$$

where ρ, u, p, p_0 and n represent density, velocity vector, pressure, ambient pressure and normal unit vector, respectively. According to the scheme in Figure 1a, the axis of the nozzle is assumed inclined
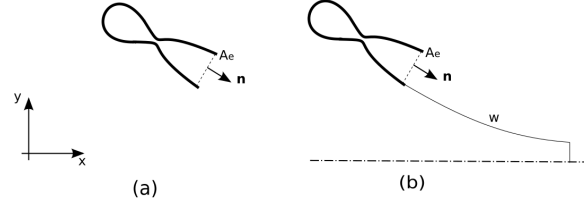
Figure 1: Scheme for the computation of the thrust component in a inclined bell nozzle (a) and in an aerospike represented by an inclined bell nozzle followed by a plug (b).

with respect to the global reference system (x, y).

Consider now a linear aerospike nozzle as represented in Fig. 1b: the Figure shows only the upper half because of symmetry considerations. The previous expression can be updated in order to compute the force in the new configuration:

$$F = \int_{A_e} (\rho(u \cdot n)u + (p - p_0)n)dA + \int_{w} ((p - p_0)\mathbb{I} + \tau) \cdot n dA \qquad (2)$$

where $\mathbb{I}$ represents the identity matrix and τ is the viscous stress tensor at wall. The first integral in Eq. 2 represents the thrust of a rocket with a nozzle truncated at the section A_e. This term is augmented by the force that the fluid applies to the plug which contains both pressure and viscous contributions. Since the aerospike is symmetric the integrals which appear in Eq. 2 must be extended to both the nozzle exits and to the full plug surface.

The terms in Eq.2 put in evidence the different mechanisms which can be exploited in an aerospike nozzle to produce a lateral force component F_y. The net lateral thrust component can be computed by applying the Eq. 2 to the two nozzles of both sides of the aerospike. When shock vectoring is applied a fluid is injected on one side of the plug: this leads to an asymmetric pressure distribution on the two sides of the plug. As a consequence, the second integral which appears in Eq. 2 leads to a net lateral force component. However, the first integral in Eq. 2 does not give any contribution in this thrust vectoring strategy because the perturbations induced by the injected fluid influence only the plug region and do not affect the flow field upstream to the section A_e.

An alternative effect is exploited when differential throttling is applied. In this case a different total pressure is imposed in the combustion chambers which feed the two sides of the plug. As a consequence both the integrals which appear in Eq. 2 contributes to the generation of the lateral force components: the first integral takes into account the force contributions generated by the region upstream to the section A_e while the second integral quantifies the pressure unbalance on the two sides of the plug.

3 NUMERICAL SIMULATION SETUP

A preliminary validation of the model and a grid convergence analysis was performed [8] on the results related to a cold flow experimental test [10]. In the present simulations the fluid is assumed to be air with frozen chemical composition. The flow field is described by means of the compressible Reynolds-averaged Navier-Stokes (RANS) equations with the Spalart-Allmaras closure model [20]. An ideal gas which follows the ideal gas equation of state is assumed. The specific heat ratio is assumed constant and
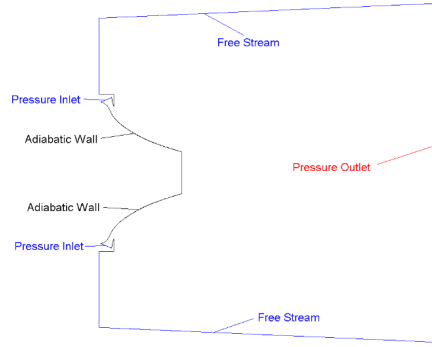
Figure 2: Computational domain.

set to $\gamma = 1.4$. The dynamic viscosity is evaluated by means of the Sutherland's law. All the simulations reported in the following were performed by assuming a nozzle pressure ratio (chamber total pressure over ambient static pressure) equal to 56.7

The governing equations are solved by means of a second order accurate finite volume discretisation implemented in the Fluent solver. Convective fluxes are evaluated by means of the Roe approximate Riemann solver [17]. The computational domain is reported in Figure 2 which shows the boundary conditions. In particular, total temperature, total pressure and angle are imposed at the nozzle inlet. The mesh contains approximately 110000 cells.

4 COMPARISON OF DIFFERENTIAL THROTTLING AND FLUIDIC THRUST VECTOR-ING

The simulations are performed on the LP40 geometry which was studied during the FESTIP program [12].

Figure 3 shows the Mach field obtained on the LP40 plug by different control strategy. In Figure 3a the results obtained by differential throttling are reported: this solution is obtained by imposing a 10% difference between the mass flow rates on the two sides. The difference is obtained by imposing different total pressure with the same total temperature.

In Figure 3b the flow field obtained by shock vector control is reported. It is possible to clearly identify the location of the secondary injection on the upper side of the plug: the secondary flow acts as an obstacle which induces a shock wave an a separation. The separation moves upstream with respect to the injection slot and generates a sort of fluidic ramp on the wall. These results refer to a ratio between the secondary and the primary mass flow rate equal to 10% and the injection slot is located at 60% of the plug lenth.

The results in Figure 3c are qualitatively similar to what observed in Figure 3b but now the injection slot is located at 90% of the plug length. The consequences induced by the choice of the injection location can be seen more clearly by comparing the wall pressure distribution which is reported in Figure 4 for both injection locations. The results show that the secondary injection generates a shock wave in front of the injection slot. The shock wave is not exactly located on the injection slot but is placed upstream because of the boundary layer separation. fact is that an expansion region is present downstream to the injection slot. The magnitude of the lateral force component is determined by the integral of the wall pressure distribution on the full plug: the compression and the expansion regions lead to opposite contri-

butions which tend to cancel each other. This effect is particularly evident when the injection is located at 60% of the plug length (see Figure 4a). In contrast, when the injection is performed at 90 % of the plug length, the surface interested by the expansion is reduced, as shown by Figure 4b.

These qualitative considerations are confirmed by the quantitative force evaluations reported in the plot of Figure 5a. In particular, the lateral thrust component normalised with respect to the magnitude of the unperturbed thrust is shown as a function of the secondary mass flow rate percentage. When the injection is performed at 90% of the plug length the behaviour is monotone and the lateral thrust component is always higher with respect to the results obtained when the injection is performed at 60% of the plug length. This seems to be related to the fact that, when the injection is performed close to the end, the expansion acts on a small region and is not able to significantly reduced the effects generated by the compression. These results are in line with the experimental finding of [5].
Furthermore, when the injection is performed at 60% of the plug length the results are non-monotone with respect to the secondary mass flow rate percentage: this could be again related to the absence of a clear net effect since both compression and expansion can influence a significant portion of the plug.

Finally, the lateral thrust component obtained by differential throttling is reported in Figure 5b: the trend in this case is very clear. The lateral thrust component grows linearly with the difference between the mass flow rates in the nozzles on the two sides of the plug.

5 CONCLUSIONS

Differential throttling and shock vectoring are investigated as possible technologies for providing thrust vectoring in an aerospike nozzle. Differential throttling is a very effective strategy which provides a lateral thrust components which varies linearly with respect to the difference between the total pressure in the chambers which feed the two sides of the spike.
Fluidic thrust vectoring and in particular shock vectoring represents a valid alternative which could be considered when differential throttling cannot be applied because a common combustion chamber is adopted: this configuration could be chosen in small scale engines. The numerical results show that shock vectoring is quite effective since it is possible to generate a significant lateral thrust component by injecting a few percentage points of the primary mass flow. The simulations show that the location of the secondary injection is a key parameter for two reasons. The first reason is that the injection induces a compression upstream to the injection slot and an expansion downstream to the injection slot: if the slot is located far from the end of the plug then the two effects tend to cancel each other and this reduces the magnitude of the lateral thrust component. This numerical result is in line with the experimental findings of [5] who underlined the importance of placing the injection slot close to the end of the plug.
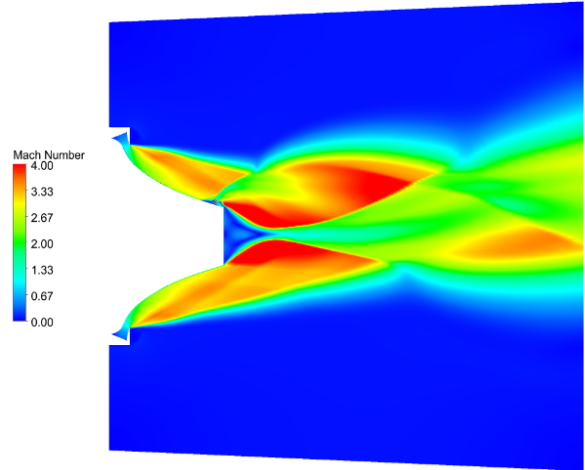
REFERENCES

[1] C. BACH, S. SCHÖNGARTH, B. BUST, M. PROPST, J. SIEDER-KATZMANN, AND M. TAJMAR, *How to steer an aerospike*, in 69th International Astronautical Congress (IAC), Bremen, Germany, 2018.

[2] E. BESNARD, H. H. CHEN, T. MUELLER, AND J. GARVEY, *Design, manufacturing and test*
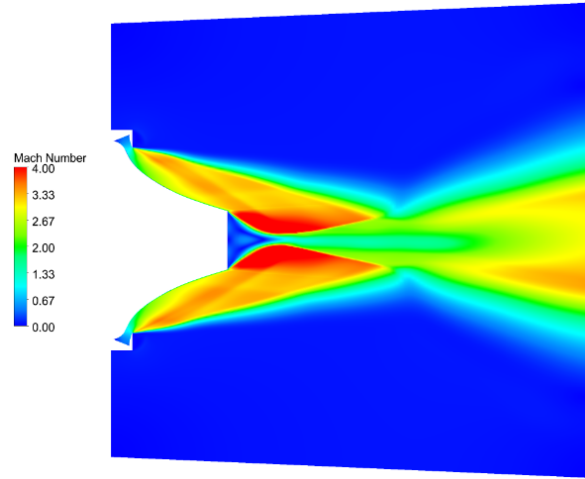
(a)
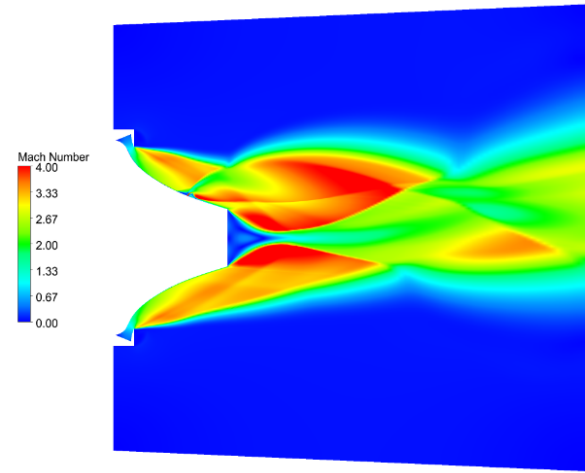
(b)

(c)

Figure 3: Mach field for LP40 with differential throttling with $\dot{m}_2/\dot{m}_1 = 0.1$ (a), SVC at $x/L = 0.6$ with $\dot{m}_i/m_1$ (b) and SVC at $x/L = 0.9$ with $\dot{m}_i/m_1 = 0.1$ (c).
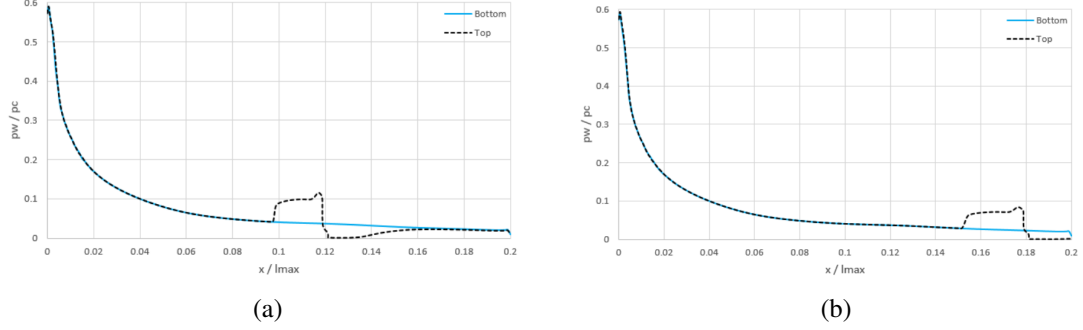
(a)   (b)

Figure 4: Wall pressure distribution on LP40 with $\dot{m}_i/m_1 = 0.1$ with injection slot at $x/L = 0.6$ (a) and $x/L = 0.9$ (b).
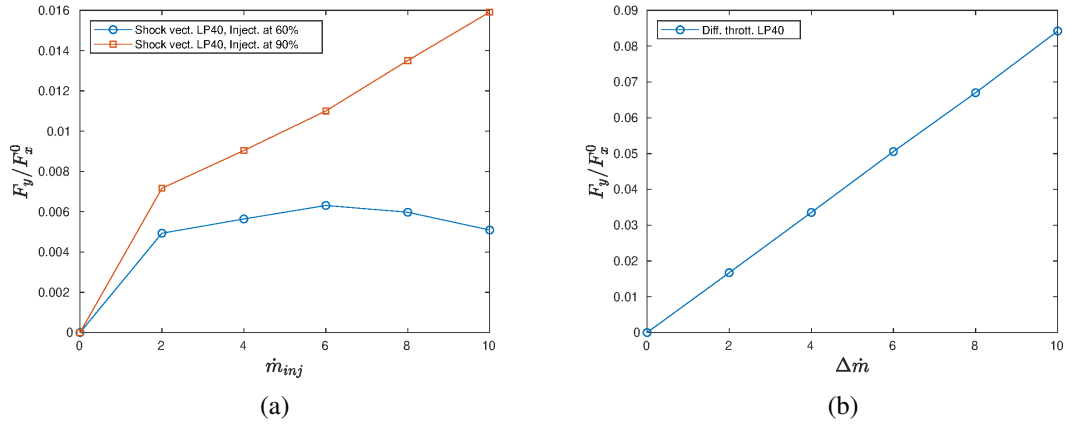

(a)   (b)

Figure 5: Side force component obtained by shock vector control (a) and differential throttling (b) on LP40 geometry.

of a plug nozzle rocket engine, in 38th AIAA/ASME/SAE/ASEE Joint Propulsion Conference & Exhibit, 2002, p. 4038.

[3] M. G. DAGOSTINO, Y. C. LEE, T.-S. WANG, AND J. TURNER, *X-33 xrs-2200 linear aerospike engine sea level plume radiation*, 2001. Technical report.

[4] G. DUMNOV, G. NIKULIN, AND N. PONOMARYOV, *Investigation of advanced nozzles for rocket engines*, Space Rocket Engines and Power Plants, 4 (1993), pp. 10–12.

[5] S. EILERS, W. MATTHEW, AND S. WHITMORE, *Analytical and experimental evaluation of aerodynamic thrust vectoring on an aerospike nozzle*, in 46th AIAA/ASME/SAE/ASEE Joint Propulsion Conference & Exhibit, 2010, p. 6964.

[6] S. D. EILERS, M. D. WILSON, S. A. WHITMORE, AND Z. W. PETERSON, *Side-force amplification on an aerodynamically thrust-vectored aerospike nozzle*, Journal of Propulsion and Power, 28 (2012), pp. 811–819.

[7] N. ERNI, *Closed-loop attitude control using fluid dynamic vectoring on an aerospike nozzle*, 2011. Thesis, Utah State University.

[8] M. FERLAUTO, A. FERRERO, AND R. MARSILIO, *Shock vector control technique for aerospike nozzles*, in AIAA Scitech 2020 Forum, 2020, p. 2246.

[9] M. FERLAUTO AND R. MARSILIO, *Numerical investigation of the dynamic characteristics of a dual-throat-nozzle for fluidic thrust-vectoring*, AIAA Journal, 55 (2017), pp. 86–98.

[10] G. HAGEMANN, H. IMMICH, T. VAN NGUYEN, AND G. E. DUMNOV, *Advanced rocket nozzles*, Journal of Propulsion and Power, 14 (1998), pp. 620–634.

[11] Z. HAO, H. TIAN, Z. GUO, L. HEDONG, AND C. LI, *Numerical and experimental investigation of throttleable hybrid rocket motor with aerospike nozzle*, Aerospace Science and Technology, 106 (2020), p. 105983.

[12] H. IMMICH, M. CAPORICCI, H. IMMICH, AND M. CAPORICCI, *Status of the festip rocket propulsion technology programme*, in 33rd Joint Propulsion Conference and Exhibit, 1997, p. 3311.

[13] D. MANSKI, *Clustered plug nozzles for future european reusable rocket launchers*, German Aerospace Research Establishment, (1981), pp. 643–81.

[14] R. MARSILIO, M. FERLAUTO, AND M. H. HAMEDI-ESTAKHRSAR, *Numerical simulation of a vectored axisymmetric nozzle*, in AIP Conference Proceedings, vol. 2293, AIP Publishing LLC, 2020, p. 200018.

[15] M. PROPST, J. SIEDER, C. BACH, AND M. TAJMAR, *Numerical analysis on an aerodynamically thrust-vectored aerospike nozzle*, in Proceedings of the 63rd German Aerospace Congress (DGLR), Augsburg, 2014.

[16] P. REIJASSE AND B. GORBEL, *Experimental analysis of the supersonic flow confluence past a jet-on axisymmetric afterbody*, in 14th Applied Aerodynamics Conference, 1996, p. 2449.

[17] P. L. ROE, *Approximate riemann solvers, parameter vectors, and difference schemes*, Journal of computational physics, 43 (1981), pp. 357–372.

[18] J. SIEDERA, C. BACH, M. PROPSTC, AND M. TAJMAR, *Evaluation of the performance potential*

of aerodynamically thrust vectored aerospike nozzles, in 67th International Astronautical Congress (IAC), Guadalajara, Mexico, 26-30 September 2016, 2016.

[19] R. SILVER, *Advanced aerodynamic spike configurations*, tech. rep., Rocketdyne, Canoga Park, United States, 1966.

[20] P. SPALART AND S. ALLMARAS, *A one-equation turbulence model for aerodynamic flows*, Recherche Aerospatiale, 1 (1994), pp. 5–21.

[21] H. TAKAHASHI, S. TOMIOKA, N. SAKURANAKA, T. TOMITA, K. KUWAMORI, AND G. MASUYA, *Experimental study on the aerodynamic performance of clustered linear aerospike nozzles*, in 18th AIAA/3AF International Space Planes and Hypersonic Systems and Technologies Conference, 2012, p. 5933.

[22] T. TOMITA, H. TAMURA, AND M. TAKAHASHI, *An experimental evaluation of plug nozzle flow field*, in 32nd Joint Propulsion Conference and Exhibit, 1996, p. 2632.